The Tom40 assembly process probed using the attachment of different intramitochondrial sorting signals

Takuya Shiota[a,*], Miyuki Maruyama[a,*], Mami Miura[a,*], Yasushi Tamura[a,*], Koji Yamano[a,†], Masatoshi Esaki[a,‡], and Toshiya Endo[a,b]

[a]Department of Chemistry, Graduate School of Science, and [b]Structural Biology Research Center, Nagoya University, Chikusa-ku, Nagoya 464-8602, Japan

ABSTRACT **The TOM40 complex is a protein translocator in the mitochondrial outer membrane and consists of several different subunits. Among them, Tom40 is a central subunit that constitutes a protein-conducting channel by forming a β-barrel structure. To probe the nature of the assembly process of Tom40 in the outer membrane, we attached various mitochondrial presequences to Tom40 that possess sorting information for the intermembrane space (IMS), inner membrane, and matrix and would compete with the inherent Tom40 assembly process. We analyzed the mitochondrial import of those fusion proteins in vitro. Tom40 crossed the outer membrane and/or inner membrane even in the presence of various sorting signals. N-terminal anchorage of the attached presequence to the inner membrane did not prevent Tom40 from associating with the TOB/SAM complex, although it impaired its efficient release from the TOB complex in vitro but not in vivo. The IMS or matrix-targeting presequence attached to Tom40 was effective in substituting for the requirement for small Tim proteins in the IMS for the translocation of Tom40 across the outer membrane. These results provide insight into the mechanism responsible for the precise delivery of β-barrel proteins to the outer mitochondrial membrane.**

Monitoring Editor
Thomas D. Fox
Cornell University

Received: Mar 11, 2012
Revised: Aug 20, 2012
Accepted: Aug 22, 2012

INTRODUCTION

Mitochondria are essential eukaryotic organelles and consist of four compartments—the outer membrane, intermembrane space (IMS), inner membrane, and innermost matrix. Mitochondria possess translocator complexes in the outer and inner membranes to import most of their resident proteins from their site of synthesis, the cytosol. The major entrance for protein import into the mitochondria is the TOM40 complex located in the outer membrane. Proteins that traverse the outer membrane through the TOM40 complex are further sorted to intramitochondrial compartments via several different translocator complexes in the outer and inner membranes (Neupert and Herrmann, 2007; Chacinska *et al.*, 2009; Endo and Yamano, 2009). The translocator complexes function as receptors to recognize mitochondrial-targeting and/or intramitochondrial sorting signals and form protein-conducting channels allowing mitochondrial precursor proteins to cross the hydrophobic barrier of the mitochondrial membranes. For instance, the TOM40 complex possesses receptor subunits including Tom20, Tom22, and Tom70 (Brix *et al.*, 1999; Abe *et al.*, 2000) and a protein-conducting channel mainly consisting of Tom40 (Hill *et al.*, 1998; Ahting *et al.*, 2001).

The mitochondrial outer membrane contains β-barrel membrane proteins, including Tom40, which require a specific translocator system for their assembly (Pfanner *et al.*, 2004; Paschen *et al.*, 2005; Imai *et al.*, 2008). Mitochondrial β-barrel proteins are synthesized in the cytosol and do not possess a cleavable N-terminal presequence. These proteins first interact with the TOM40 complex for recognition

This article was published online ahead of print in MBoC in Press (http://www.molbiolcell.org/cgi/doi/10.1091/mbc.E12-03-0202) on August 29, 2012.

*These authors contributed equally to this work.

Present addresses: †Biochemistry Section, Surgical Neurology Branch, National Institute of Neurological Disorders and Stroke, National Institutes of Health, Bethesda, MD 20892; ‡Division of Molecular Cell Biology, Institute of Molecular Embryology and Genetics, Kumamoto University, 2-2-1 Honjo, Kumamoto 860-0811, Japan.

Address correspondence to: Toshiya Endo (endo@chem.nagoya-u.ac.jp).

Abbreviations used: BN-PAGE, blue-native PAGE; EM, electron microscopy; HBD, heme-binding domain; Imp1, inner-membrane protease 1; IMS, intermembrane space; MPP, mitochondrial processing peptidase; PK, proteinase K; $\Delta\Psi$, membrane potential across the inner membrane; WT, wild type.

of their internal targeting signals and then translocate across the outer membrane (Wiedemann *et al.*, 2003). Assembly of the proteins into the outer membrane involves antiparallel β-strands forming a barrel structure, and this requires another translocator in the outer membrane, the TOB/SAM complex, which consists of Sam37/Mas37/Tom37 (Wiedemann *et al.*, 2003), Sam50/Tob55 (Kozjak *et al.*, 2003; Paschen *et al.*, 2003; Gentle *et al.*, 2004), and Sam35/Tom38/Tob38 (Ishikawa *et al.*, 2004; Milenkovic *et al.*, 2004; Waizenegger *et al.*, 2004a). In addition, small Tim proteins in the IMS are also needed for the early step of β-barrel protein assembly (Hoppins and Nargang, 2004; Wiedemann *et al.*, 2004), and Tom40 requires another outer membrane protein, Tom13/Mim1, in the later stage of its assembly process (Ishikawa *et al.*, 2004; Waizenegger *et al.*, 2004b). Mdm10, which is involved in the tethering complex for mitochondrial and endoplasmic reticulum membranes (Kornmann *et al.*, 2009), as well as in the TOB complex (Meisinger *et al.*, 2004), also facilitates the assembly of Tom40, or more specifically controls when Tom40 exits the TOB complex (Yamano *et al.*, 2010a,b). Despite the identification of the components mediating the β-barrel protein assembly, there remain many questions as to the precise roles of these components in the sorting and assembly of β-barrel proteins such as Tom40.

Here we designed an experimental system to generate competitive or tug-of-war situations in investigating the sorting and assembly of Tom40 in the outer membrane. This was achieved by attaching sorting signals for submitochondrial compartments other than the outer membrane to Tom40. We chose the presequence of the precursor to a soluble IMS protein, cytochrome b_2, and its derivatives as tools to perturb the sorting pathway of Tom40. The cytochrome b_2 presequence exhibits a bipartite structure: the N-terminal part functions as a targeting signal for the mitochondrial matrix, and the C-terminal part mediates sorting to the IMS (Glick *et al.*, 1992; Esaki *et al.*, 1999). The N-terminal portion reaches the matrix via the TOM40 complex and the TIM23 complex with the aid of the membrane potential across the inner membrane ($\Delta\Psi$) and mitochondrial Hsp70 in the matrix and is proteolytically cleaved by the mitochondrial processing peptidase (MPP) in the matrix. The C-terminal part of the presequence then arrests translocation of the presequence through the TIM23 complex and is cleaved off by the inner-membrane protease 1 (Imp1) on the IMS side of the inner membrane after lateral release from the TIM23 complex into the inner membrane. A cytochrome b_2 presequence derivative with an inactivated sorting signal (such as the $pb_2\Delta19$ presequence, which lacks 19 residues in the sorting signal) cannot arrest the presequence translocation across the inner membrane, which means that it directs the passenger protein to the matrix. When Imp1 processing of the cytochrome b_2 presequence is inhibited by mutations in the cleavage site of the presequence, the passenger protein cannot be released into the IMS but instead remains anchored to the inner membrane (Esaki *et al.*, 1999).

In the present study, we performed in vitro mitochondrial import of fusion proteins consisting of Tom40 N-terminally attached to cytochrome b_2–derived and other presequences with sorting signals for the matrix, inner membrane, and IMS. The results show that the pathway for Tom40 assembly in the outer membrane is not exclusive to the inner membrane or IMS sorting pathway, but that it is separate from the $\Delta\Psi$-dependent matrix-targeting pathway. When import of Tom40 was directed by the inner membrane or IMS-sorting presequences, the requirement of small Tim proteins for the assembly of Tom40 was partially circumvented. The import properties of the Tom40-containing fusion proteins revealed in vitro were also found to be consistent with their behaviors in vivo, except for Tom40 with an inner-membrane anchored presequence, which was efficiently assembled into the final TOM40 complex in vivo but not in vitro.

RESULTS

pb_2(220)-Tom40 follows the normal Tom40 assembly pathway in the outer membrane

We generated fusion proteins between the N-terminal part of the cytochrome b_2 precursor or its derivatives and Tom40 as shown in Figure 1. pb_2(220)-Tom40 contains the N-terminal 220 residues of the cytochrome b_2 precursor, followed by Tom40. pb_2(220)Δ19-Tom40 contains a deletion of residues 47–65 (Δ19), which inactivates the IMS sorting signal in the cytochrome b_2 presequence. pb_2(220)AA-Tom40 contains the mutations N80A and E81A, which abolish the presequence cleavage site for Imp1. pb_2(220)dc1-Tom40 and pb_2(220)dc2-Tom40 contain the dc1 and dc2 mutations in the heme-binding domain (HBD; residues 81–180) of cytochrome b_2, which lead to destabilization of the HBD and thereby retard Imp1 processing (Esaki *et al.*, 1999).

We synthesized these fusion proteins in rabbit reticulocyte lysate in the presence of [^{35}S]methionine and compared their in vitro import into isolated yeast mitochondria with that of Tom40 (Figures 2 and 3). When incubated with energized mitochondria at 25°C, Tom40 was imported into mitochondria and became resistant to proteinase K (PK) added outside the mitochondria (Figure 2A, +PK). The presequence of pb_2(220)-Tom40 was subject to two-step processing during incubation with energized mitochondria, and both the intermediate-size form (i) and mature size form (m), but not the precursor form (p), became PK resistant (Figure 2A, +PK). Therefore, despite the attachment of Tom40, the cytochrome b_2 presequence was correctly cleaved by MPP in the matrix and subsequently by Imp1 in the IMS, suggesting that the N-terminus of the imported and processed pb_2(220)-Tom40 was exposed to the IMS.

We then probed the fate of the C-terminal Tom40 domain of pb_2(220)-Tom40 in the IMS after the second Imp1 cleavage of the presequence. The assembly process of imported Tom40 in the outer membrane can be analyzed using blue native-PAGE (BN-PAGE; Model *et al.*, 2001). After incubation of Tom40 or pb_2(220)-Tom40 with isolated mitochondria, the mitochondria were solubilized with 1% digitonin and subjected to BN-PAGE analyses. BN-PAGE results showed that Tom40 was assembled into the 450-kDa TOM40 complex via two successive intermediates of a ~250-kDa complex (assembly I), which often exhibit two bands that migrate at slightly different molecular sizes on the gel, and a 100-kDa complex (assembly II; Figure 2B). Of interest, pb_2(220)-Tom40 exhibited a similar

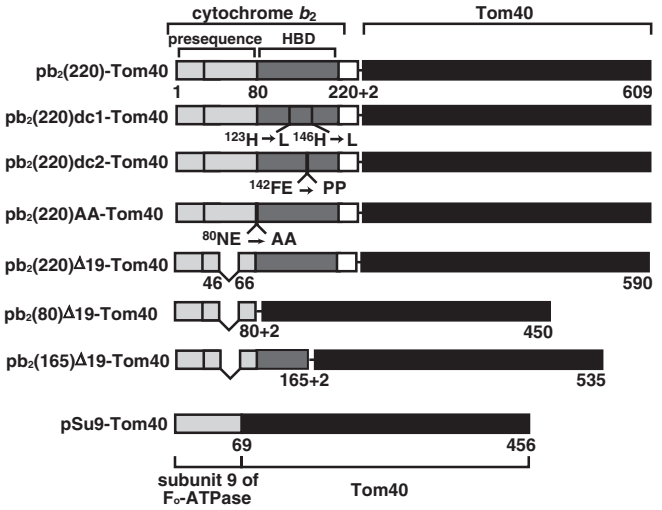

FIGURE 1: Tom40 fusion proteins used in the present study.

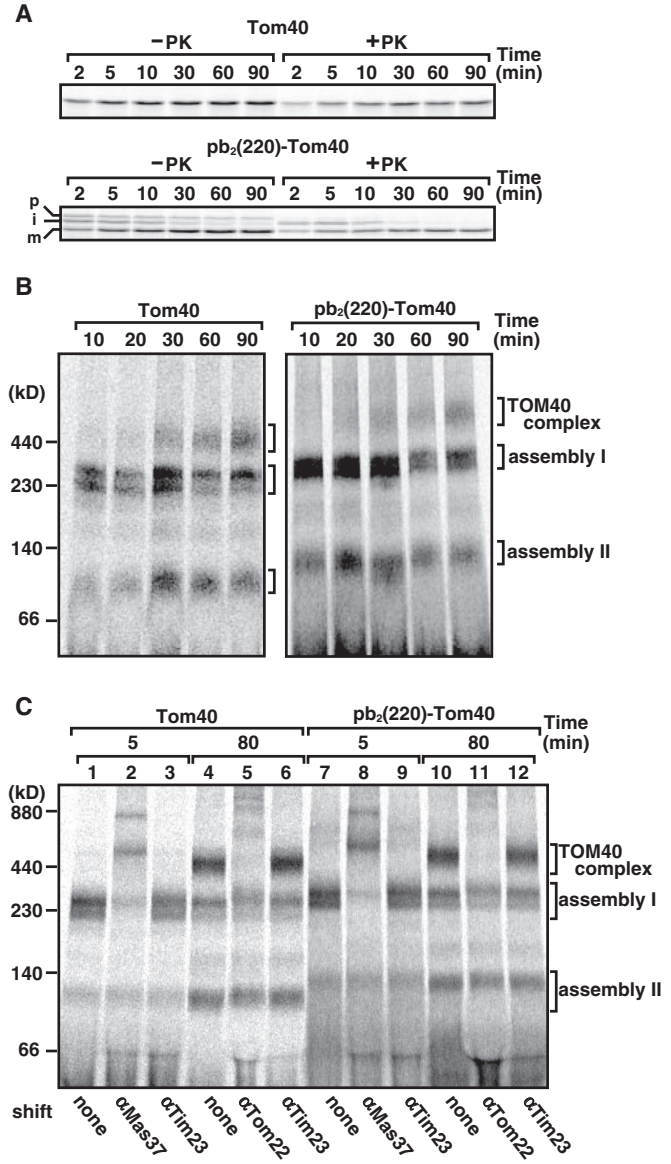

FIGURE 2: In vitro import of Tom40 and pb_2(220)-Tom40. (A) ^{35}S-labeled proteins were incubated with isolated yeast mitochondria at 25°C for indicated times. The mitochondria were treated with or without PK, and proteins were analyzed by SDS–PAGE and radioimaging. i, intermediate-size form; m, mature-size form; p, precursor form. (B) The mitochondria in A (−PK) were solubilized with 1% digitonin and subjected to BN-PAGE and radioimaging. (C) ^{35}S-labeled proteins were imported into isolated yeast mitochondria for 5 or 80 min at 25°C. After reisolation, the mitochondria were solubilized with 1% digitonin, incubated with the antibodies against Sam37/Mas37 (αMas37), Tim23 (αTim23), or Tom22 (αTom22) or without antibodies (none) for 60 min at 4°C, and analyzed by BN-PAGE and radioimaging. (D) ^{35}S-labeled proteins were imported into yeast mitochondria with FLAG-tagged Sam50/Tob55 for 5 min at 25°C. BN-PAGE with the antibody shift was performed as in C by using the anti-FLAG antibody. The shifted bands are indicated by white arrowheads.

assembly pattern, although the apparent molecular sizes of the assembly intermediates and the final TOM40 complex were slightly larger than those observed for Tom40, probably due to the larger molecular size of pb_2(220)-Tom40 compared with Tom40 (Figure 2B). We confirmed, by observing an antibody shift on a BN-PAGE gel, that the assembly I–like band of pb_2(220)-Tom40 indeed represents the assembly I intermediate involving the TOB complex as observed for Tom40. Addition of antibodies against Sam37/Mas37, a subunit of the TOB complex, shifted the assembly I–like band to a higher molecular mass range on the BN-PAGE gel (Figure 2C, lane 8). We observed a similar shift of the assembly I–like band of pb_2(220)-Tom40 upon addition of the anti-FLAG antibody when we used mitochondria with FLAG-tagged Sam50/Tob55 (Figure 2D, lane 4). We also confirmed that the TOM40 complex–like band of pb_2(220)-Tom40 corresponded to the final TOM40 complex, since addition of antibodies against Tom22, a subunit of the TOM40 complex, shifted the band to a higher molecular mass range (Figure 2C, lane 11). These results suggest that, whereas the cytochrome b_2 presequence of pb_2(220)-Tom40 is processed in the matrix and IMS sequentially along the normal sorting pathway for the cytochrome b_2 precursor, the C-terminally attached Tom40 part can follow its normal assembly pathway via the two intermediates, assembly I and assembly II, to the final TOM40 complex in the outer membrane. In other words, the two distinct sorting signals in the cytochrome b_2 presequence and Tom40 do not interfere with each other with respect to their in vitro import assay.

The second presequence processing of pb_2(220)-Tom40 is not a prerequisite for formation of the assembly I intermediate

Because assembly of the Tom40 part of pb_2(220)-Tom40 into the outer membrane is a slow process compared with the presequence processing of the cytochrome b_2 precursor part, it is not clear whether the presequence processing triggers assembly of Tom40 in the outer membrane after entering the IMS. We thus analyzed the in vitro mitochondrial import of pb_2(220)Δ19-Tom40 and pb_2(220)AA-Tom40 without the second presequence cleavage site (Esaki *et al.*, 1999), as well as the mitochondrial import of pb_2(220)dc1-Tom40 and pb_2(220)dc2-Tom40, which undergo retarded second presequence processing (Esaki *et al.*, 1999).

When pb_2(220)Δ19-Tom40 and pb_2(220)AA-Tom40 were incubated with mitochondria at 25°C, the precursor forms were rapidly converted to protease-resistant intermediate-size forms by MPP processing of the presequence, but the mature-size forms were not generated as expected (Figure 3A). The amount of imported protease-resistant pb_2(220)Δ19-Tom40 slowly decreased (Figure 3A), suggesting that it was degraded inside the mitochondria. pb_2(220)dc1-Tom40 and pb_2(220)dc2-Tom40 were also rapidly converted to the protease-resistant intermediate size forms, but, in contrast to pb_2(220)AA-Tom40, the intermediate-size forms subsequently

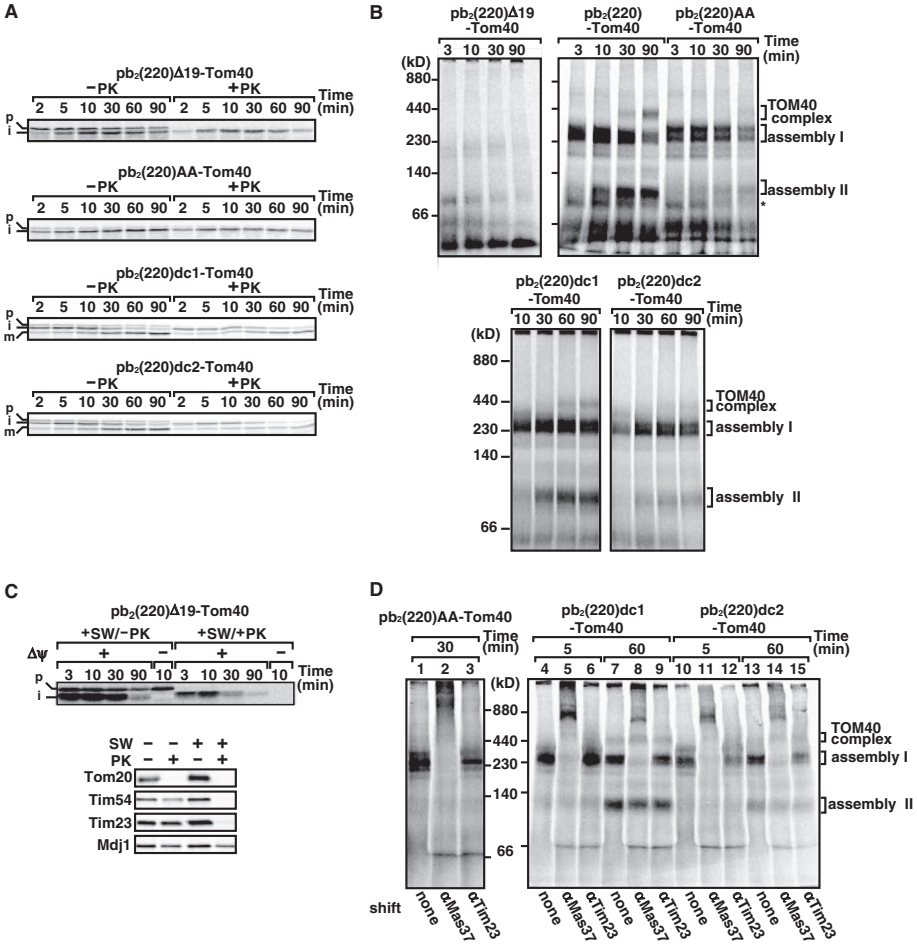

FIGURE 3: In vitro import of $pb_2(220)\Delta19$-Tom40, $pb_2(220)$AA-Tom40, $pb_2(220)$dc1-Tom40, and $pb_2(220)$dc2-Tom40. (A) ^{35}S-labeled proteins were imported into isolated yeast mitochondria and analyzed as in Figure 2A. i, intermediate-size form; m, mature-size form; p, precursor form. (B) The mitochondria in A (–PK) were solubilized with 1% digitonin and subjected to BN-PAGE. Asterisk, unspecific band. (C) Top, ^{35}S-labeled $pb_2(220)\Delta19$-Tom40 was incubated with isolated mitochondria at 25°C for indicated times. The mitochondria were then subjected to osmotic swelling (SW) and treated with or without PK. The mitochondria (–SW) or mitoplasts (+SW) were reisolated by centrifugation, and proteins were analyzed by SDS–PAGE and radioimaging. Bottom, mitochondria (–SW) or mitoplasts (+SW) generated by osmotic swelling were treated with or without PK. Proteins were analyzed by immunoblotting with antibodies against indicated proteins. (D) ^{35}S-labeled indicated proteins were imported into isolated yeast mitochondria for indicated times at 25°C. After reisolation, the mitochondria were solubilized with 1% digitonin, incubated with antibodies against Sam37/Mas37 (αMas37) and Tim23 (αTim23) or without antibodies (none) for 60 min at 4°C, and analyzed by BN-PAGE and radioimaging.

underwent slow second processing of the presequence by Imp1 to become mature-size forms, albeit at slower rates than $pb_2(220)$-Tom40 (Figure 3A), as shown previously for $pb_2(220)$dc1 and $pb_2(220)$dc2 fusion proteins (Esaki *et al.*, 1999).

We then analyzed the fate of imported $pb_2(220)\Delta19$-Tom40, $pb_2(220)$AA-Tom40, $pb_2(220)$dc1-Tom40, and $pb_2(220)$dc2-Tom40 inside mitochondria by solubilizing mitochondria with digitonin, followed by BN-PAGE. The assembly of Tom40 into the outer membrane via the assembly I and II intermediates was markedly inhibited when we replaced the $pb_2(220)$ presequence with the $pb_2(220)\Delta19$ presequence (Figure 3B, top), suggesting that imported $pb_2(220)\Delta19$-Tom40 was not sorted to the outer membrane. We thus asked whether imported $pb_2(220)\Delta19$-Tom40 reached the matrix instead of the outer membrane via the matrix-targeting Δ19 presequence. In the presence of ΔΨ, imported $pb_2(220)\Delta19$-Tom40, like the mitochondrial matrix protein Mdj1, was partly resistant to PK digestion even after opening of the outer membrane by osmotic swelling, whereas Tom20 in the outer membrane and Tim54 and Tim23 in the inner membrane facing the IMS were susceptible to PK digestion in mitochondria and in mitoplasts, respectively (Figure 3C). This indicates that a major fraction of the $pb_2(220)\Delta19$-Tom40 protein underwent presequence processing by MPP; that the Tom40 moiety was at least partly sequestered into the matrix; and that the $pb_2(220)\Delta19$ presequence could partially direct the attached Tom40 moiety to the matrix. When we tested the import of the matrix-targeting Δ19 presequence alone ($pb_2(80)\Delta19$-Tom40) or one followed by the N-terminal 85 residues of cytochrome b_2 lacking the HBD ($pb_2(165)\Delta19$-Tom40), most fractions of the $pb_2(80)\Delta19$-Tom40 and $pb_2(165)\Delta19$-Tom40 proteins reached the matrix (Supplemental Figure S1A). Therefore $pb_2(220)\Delta19$-Tom40 with the HBD, but not $pb_2(80)\Delta19$-Tom40 or $pb_2(165)\Delta19$-Tom40, may be mainly stalled at the TIM23 complex in a tug-of-war between forces that target the Tom40 moiety to the outer membrane and forces that translocate the presequence into the matrix by unfolding the tightly folded HBD. Indeed, when we inactivated the import motor, mitochondrial Hsp70, by depletion of Tim15/Hep1 (Sichting *et al.*, 2006; Momose *et al.*, 2007) in the presence of ΔΨ (Supplemental Figure S1B), a minor fraction of the $pb_2(220)\Delta19$-Tom40 protein escaped the matrix-targeting pathway and was partially captured by the Tom40 assembly pathway (Supplemental Figure S1C).

On the other hand, $pb_2(220)$AA-Tom40, $pb_2(220)$dc1-Tom40, and $pb_2(220)$dc2-Tom40 appeared to partly follow the Tom40 assembly pathway, as shown by their migration on BN-PAGE gels (Figure 3B). The assembly I–like form observed during the assembly of $pb_2(220)$AA-Tom40 (Figure 3B, top) was shifted to a higher molecular mass range upon addition of anti-Mas37 antibodies (Figure 3D, lane 2). However, in contrast to $pb_2(220)$-Tom40, conversion of the assembly I intermediate of $pb_2(220)$AA-Tom40 to the assembly II form was impaired (Figure 3B, top). Therefore the intermediate-size form of $pb_2(220)$AA-Tom40, which was presumably anchored to the inner membrane through the uncleaved C-terminal half of its presequence, was partly assembled into the TOB complex to form the assembly I intermediate but was not efficiently released from the TOB complex to proceed further along the assembly pathway of Tom40.

BN-PAGE analysis showed that $pb_2(220)$dc1-Tom40 and $pb_2(220)$dc2-Tom40, which exhibited slow second presequence processing, had retarded assembly of the Tom40 domain (Figure 3B, bottom). The assembly I intermediates were associated with the TOB complex, as they were all shifted to a higher molecular mass range by the addition of anti-Mas37 antibodies (Figure 3D, lanes 5, 8, 11, and

14). In contrast to pb_2(220)AA-Tom40, both pb_2(220)dc1-Tom40 and pb_2(220)dc2-Tom40 exhibited bands representing the 100-kDa assembly II–like forms and the 450-kDa final TOM40 complex (Figure 3B, bottom), indicating that they continued along the assembly pathway for Tom40 past its assembly into the assembly I intermediate in the outer membrane once they had undergone second Imp1 processing of the presequence.

N-terminal anchoring to the inner membrane partly replaces the role of small Tim proteins in the translocation of Tom40 across the outer membrane

It was suggested that small Tim proteins in the IMS facilitate the assembly of Tom40 into the outer membrane, since depletion of Tim8 and Tim13 (Hoppins and Nargang, 2004) or expression of functionally defective Tim10 (Wiedemann *et al.*, 2004) suppresses the assembly of Tom40 into the assembly I intermediate, although the assembly II intermediate and the final TOM40 complex are still partially formed (Wiedemann *et al.*, 2004). We thus asked whether attachment of the cytochrome b_2 presequence to Tom40 would alter the requirement of small Tim proteins for the correct assembly of the Tom40 part in the outer membrane. For this purpose, we used a yeast strain (GAL-TIM10) in which the galactose-inducible *GAL7* promoter was integrated into the chromosome in front of the *TIM10* gene to achieve regulated expression of Tim10 by galactose (Yamano *et al.*, 2005). Thirteen hours after the shift from galactose-containing medium to glucose-containing medium, mitochondria isolated from the GAL-TIM10 cells showed a significantly reduced level of Tim10, whereas levels of the subunits of the other translocators were not affected (Figure 4A).

We prepared mitochondria from the Tim10-depleted cells (Tim10↓) and tested their ability to import pb_2(220)-Tom40. Because Tim10 is also involved in the transfer of inner membrane carrier proteins from the TOM40 complex to the TIM22 complex in the inner membrane (Koehler *et al.*, 1998; Sirrenberg *et al.*, 1998), we confirmed that the import rate of ADP/ATP carrier, a substrate for the TIM22 pathway, but not pSu9-DHFR, a substrate for the TIM23 pathway, was significantly lowered in Tim10↓ mitochondria as compared with wild-type (WT) mitochondria (Figure 4B). Whereas import of Tom40 into mitochondria was significantly impaired by depletion of Tim10 as judged by resistance to PK treatment, import of pb_2(220)-Tom40 into mitochondria was only moderately affected (Figure 4B).

Imported Tom40 and pb_2(220)-Tom40 were then analyzed by BN-PAGE after solubilization of mitochondria with digitonin. Reflecting the reduced amount of imported Tom40, hardly any Tom40 assembly I intermediate was formed in Tim10↓ mitochondria (Figure 4C). pb_2(220)-Tom40 imported into Tim10↓ mitochondria also formed a lower amount of the assembly I intermediate; however, it formed the assembly II intermediate partly, and the level of the final TOM40 complex detected was comparable to that observed in WT mitochondria (Figure 4C). Therefore, in contrast to Tom40, pb_2(220)-Tom40 crossed the outer membrane efficiently but, in the absence of Tim10, formed the final TOM40 complex without efficiently accumulating the assembly I intermediate. This may indicate that the assembly I intermediate was destabilized or later assembly steps were somehow accelerated in the absence of Tim10.

Switching of the sorting pathways of pb_2(80)Δ19-Tom40 and pSu9-Tom40 between the matrix and outer membrane

Next we tested the effects of dissipation of $\Delta\Psi$, which is essential for presequence-containing precursor proteins to cross the inner membrane via the TIM23 channel, on the assembly of the Tom40 part of pb_2(220)-Tom40, pb_2(220)Δ19-Tom40, and pSu9-Tom40

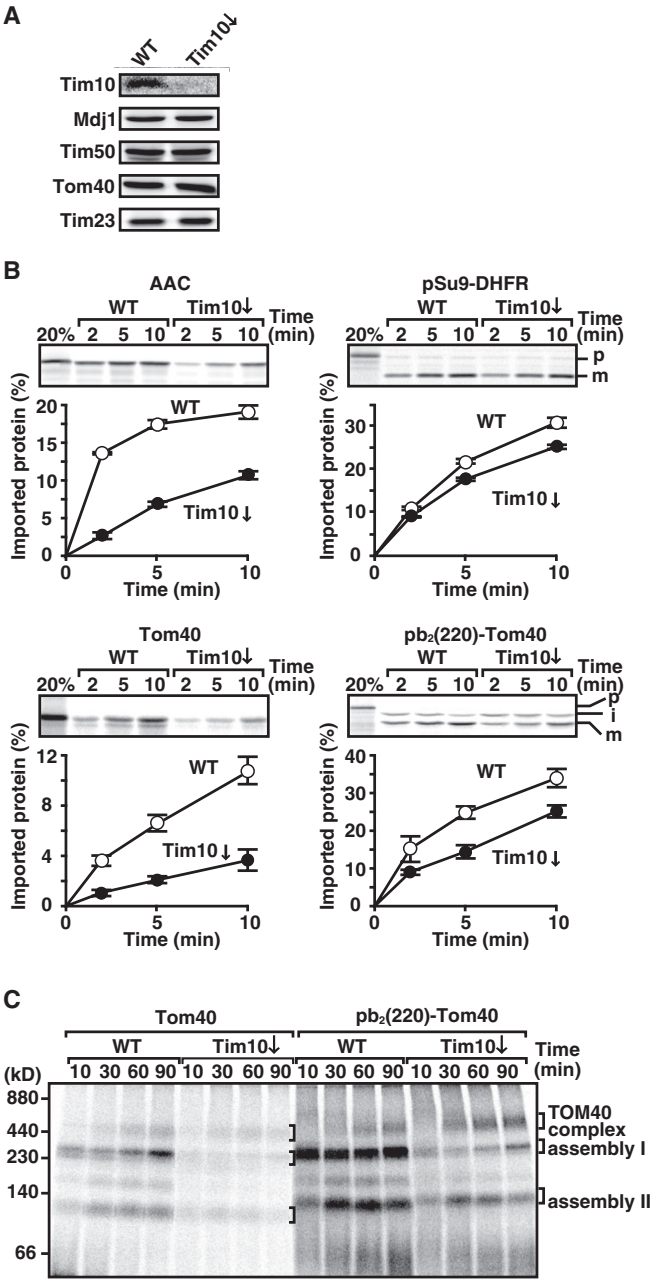

FIGURE 4: In vitro import of Tom40 and pb_2(220)-Tom40 into Tim10-depleted mitochondria. (A) Mitochondria were isolated from yeast stains W303-1A (WT) and GAL-TIM10 (Tim10↓), which were grown at 23°C for 13 h in lactate (+1% glucose) medium, and proteins were analyzed by SDS–PAGE and immunoblotting with antibodies against indicated proteins. (B) ^{35}S-labeled indicated proteins were incubated with WT and Tim10↓ mitochondria at 25°C for indicated times. The mitochondria were treated with PK, and proteins were analyzed by SDS–PAGE and radioimaging. The amounts of protease-protected forms are quantified at the bottom. The amounts of ^{35}S-labeled proteins added to each reaction are set to 100%. Values are means ± SD calculated from three independent experiments. i, intermediate-size form; m, mature-size form; p, precursor form. (C) The WT and Tim10↓ mitochondria in B (–PK) were solubilized with 1% digitonin and subjected to BN-PAGE analyses.

(a fusion protein consisting of another 69-residue matrix-targeting presequence of subunit 9 of F_o-ATPase followed by Tom40). In the presence of $\Delta\Psi$, all these fusion proteins crossed the outer

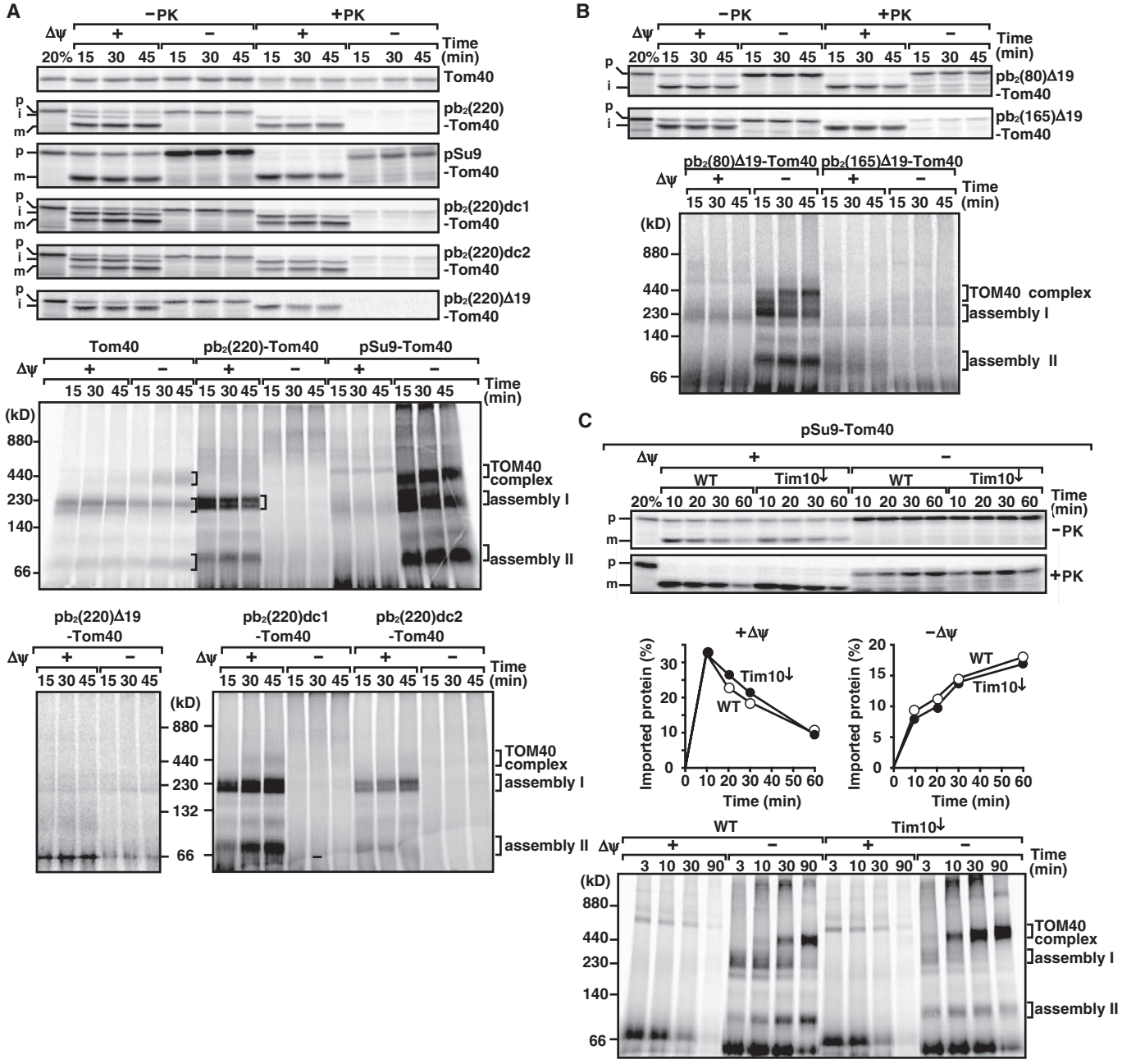

FIGURE 5: Roles of ΔΨ in import and assembly of the Tom40 fusion proteins. (A) Top, ^{35}S-labeled indicated proteins were incubated with isolated yeast mitochondria in the presence (–ΔΨ) or absence (+ΔΨ) of valinomycin at 25°C for indicated times. The mitochondria were treated with or without PK, and proteins were analyzed by SDS–PAGE and radioimaging. Middle and bottom, the mitochondria in A (–PK) were solubilized with 1% digitonin and subjected to BN-PAGE analyses. m, mature-size form; p, precursor form. (B) Top, ^{35}S-labeled proteins were imported into mitochondria in the presence (–ΔΨ) or absence (+ΔΨ) of valinomycin at 25°C for indicated times and analyzed as in A. (C) Mitochondria were isolated from W303-1A (WT) and GAL-TIM10 (Tim10↓) after cultivation in lactate (+1% glucose) medium for 13 h at 23°C. ^{35}S-labeled pSu9-Tom40 was incubated with WT and Tim10↓ mitochondria in the presence (–ΔΨ) or absence (+ΔΨ) of valinomycin at 25°C for indicated times. The mitochondria were treated with or without PK, and proteins were analyzed by SDS–PAGE and radioimaging (top) and quantified (bottom). WT and Tim10↓ mitochondria incubated with ^{35}S-labeled pSu9-Tom40 or pb_2(220)dc1-Tom40 in the presence (–ΔΨ) or absence (+ΔΨ) of valinomycin at 25°C for indicated times were solubilized with 1% digitonin and subjected to BN-PAGE analyses (bottom).

membrane to become PK resistant and had their presequences processed by MPP and/or Imp1 (Figure 5A, top). However, only pb_2(220)-Tom40, pb_2(220)dc1-Tom40, and pb_2(220)dc2-Tom40 entered the Tom40 assembly pathway in the outer membrane (Figure 5A, middle and bottom). Instead, pb_2(220)Δ19-Tom40 and pSu9-Tom40 entered the matrix-sorting pathway and were degraded in the matrix over time (Figure 5, A, top, and C, top and middle left, and Supplemental Figure S1A). In the absence of ΔΨ,

pb_2(220)-Tom40 or pb_2(220)Δ19-Tom40 could not be imported into mitochondria (Figure 5A, top), meaning that they could not enter the Tom40 assembly pathway in the outer membrane (Figure 5A, middle and bottom). By contrast, whereas the presequence was not cleaved off in the matrix, pSu9-Tom40 unexpectedly became PK-resistant after incubation with deenergized mitochondria (Figure 5A, top). The Tom40 part of pSu9-Tom40 was assembled into the final TOM40 complex via the assembly I and assembly II intermediates (Figure 5A, middle), similar to WT Tom40. Because pSu9-Tom40, which was assembled into the outer membrane, was slightly smaller after treatment with PK (Figure 5A, top), we asked which terminus of the pSu9-Tom40 protein is exposed to the cytosol. PK treatment of pSu9-Tom40 containing a 10-histidine (His_{10}) or FLAG tag at the C-terminus gave rise to slightly smaller species that contained these tags (Supplemental Figure S2), suggesting that the N-terminus, but not the C-terminus, of pSu9-Tom40 is exposed to the cytosol after assembly in the outer membrane.

We next investigated why the Tom40 part of pSu9-Tom40 can follow the Tom40 assembly pathway in deenergized mitochondria, whereas that of pb_2(220)-Tom40 or pb_2(220)Δ19-Tom40 cannot. In the absence of ΔΨ, the presequence of pb_2(220)-Tom40 or pb_2(220)Δ19-Tom40 is not cleared from the TOM40 complex for transfer to the TIM23 complex (Kanamori *et al.*, 1999). Thus the 140-residue mature part of cytochrome b_2 in front of Tom40 may well prevent access of the Tom40 part to the inlet of the TOM40 channel because of the long distance between the presequence and the Tom40 part and/or the presence of the tightly folded HBD (residues 81–180) in between. To test the effects of the tightly folded HBD, we analyzed the import of pb_2(220)dc1-Tom40 and pb_2(220)dc2-Tom40 with a destabilized HBD (Esaki *et al.*, 1999). Both destabilized fusion proteins were, like pb_2(220)-Tom40 and pb_2(220)Δ19-Tom40, neither imported into deenergized mitochondria (Figure 5A, top) nor sorted to the Tom40 assembly pathway (Figure 5A, bottom). We also confirmed that, even if the cytochrome b_2 part was shortened by 55 residues, resulting in disruption of the folded HBD, pb_2(165)Δ19-Tom40 was still not imported into mitochondria even in the absence of ΔΨ (Figure 5B). However, when the cytochrome b_2 part became as short as the presequence, the resulting fusion protein, pb_2(80)Δ19-Tom40, was imported into mitochondria in the absence of ΔΨ (Figure 5B). As observed for pb_2(220)Δ19-Tom40 and pSu9-Tom40, both pb_2(80)Δ19-Tom40 and pb_2(165)Δ19-Tom40 were imported into the matrix in the presence of ΔΨ (Supplemental Figure S1). Therefore long segments, not the tightly folded HBD domain, between the presequence and Tom40 in pb_2(220)-Tom40 and pb_2(220)Δ19-Tom40 prevent the entry of the Tom40 part into the TOM40 complex in mitochondria lacking ΔΨ.

Because the Tom40 part of pSu9-Tom40 enters the Tom40 assembly pathway without the assistance of ΔΨ, we asked whether assembly of this Tom40 domain requires small Tim proteins, which are necessary for assembly of WT Tom40. However, the translocation of pSu9-Tom40 across the inner membrane into deenergized mitochondria was not impaired by depletion of Tim10 (Figure 5C, top and middle right). Instead, pSu9-Tom40, which was imported in the absence of both ΔΨ and Tim10, formed the final TOM40 complex without accumulating the assembly I intermediate efficiently (Figure 5C, bottom). In this respect, the formation of the final TOM40 complex by pSu9-Tom40 resembled that of pb_2(220)-Tom40 (Figure 4C). Therefore, although the pSu9 presequence cannot proceed beyond interactions with the *trans* site (i.e., IMS side) of the TOM40 complex and Tim50 of the TIM23 complex in the absence of ΔΨ (Tamura *et al.*, 2009), the presence of the presequence abolishes the requirement for the small Tim proteins to cross the outer membrane.

On the other hand, the presence of Tom40 decreased the dependence of pSu9-Tom40 on the receptor functions of the TIM23 complex in the absence of ΔΨ. The *tim23-71* mutant with the L71S mutation in Tim23 exhibits defects in the import of both matrix-targeted and IMS-targeted precursor proteins because of the defective presequence-receptor function of Tim23 (Tamura *et al.*, 2009). Whereas the import of pb_2(220)-Tom40, as well as that of pSu9-DHFR, in the presence of ΔΨ was significantly retarded by the L71S mutation in Tim23 (Supplemental Figure S3A), the L71S mutation only mildly affected the import of pSu9-Tom40 into energized mitochondria (Supplemental Figure S3A, +ΔΨ) and its assembly into the final TOM40 complex in deenergized mitochondria (Supplemental Figure S3B, –ΔΨ). These results suggest that, although the receptor function of the TIM23 complex is required for the presequence-directed translocation of the Tom40 fusion protein across the outer membrane, the presence of the Tom40 part tends to decrease dependence on the TIM23 receptor.

Tom40 fusion proteins lacking a matrix-targeting signal can be correctly assembled into the TOM40 complex in vivo

We next wanted to verify whether the in vitro assembly pathway of Tom40 analyzed here is relevant to that occurring in vivo. We thus asked whether pb_2(220)-Tom40, pb_2(220)Δ19-Tom40, pb_2(220)AA-Tom40, pb_2(220)dc1-Tom40, pb_2(220)dc2-Tom40, and pSu9-Tom40 could substitute for WT Tom40 in vivo. A haploid yeast strain whose chromosomal *TOM40* disruption was complemented by a *URA3* plasmid carrying the WT *TOM40* gene was transformed with *TRP1* plasmids containing the genes for either pb_2(220)-Tom40 derivatives or pSu9-Tom40. When cells lacking the *URA3* plasmid were selected on a 5′-fluoroorotic acid (5′-FOA) plate, cells expressing pb_2(220)-Tom40, pb_2(220)AA-Tom40, pb_2(220)dc1-Tom40, or pb_2(220)dc2-Tom40, but not those expressing pb_2(220)Δ19-Tom40 or pSu9-Tom40, grew (Figure 6A). Cell extracts were prepared from the strains expressing pb_2(220)-Tom40, pb_2(220)AA-Tom40, pb_2(220)dc1-Tom40, or pb_2(220)dc2-Tom40 instead of WT Tom40 and were subjected to immunoblotting with anti-Tom40 antibodies. pb_2(220)-Tom40 exhibited a lower molecular weight band than pb_2(220)AA-Tom40, suggesting that pb_2(220)-Tom40 was correctly processed to form a mature-size form, whereas pb_2(220)AA-Tom40 was only subjected to first MPP processing of the presequence to form the intermediate-size form (Figure 6B). pb_2(220)dc1-Tom40 and pb_2(220)dc2-Tom40 exhibited two forms corresponding to the intermediate-size and mature-size forms because their second presequence processing is retarded (Figure 6B) These results show that processing of the presequences of the pb_2(220)-Tom40 variants took place in the same manner in cells as for the processing of pb_2(220)-Tom40 variants imported into isolated mitochondria in vitro and that they were functional in vivo.

Next we analyzed the assembly structure of pb_2(220)-Tom40 and pb_2(220)AA-Tom40 in vivo by BN-PAGE. Mitochondria containing pb_2(220)-Tom40, pb_2(220)AA-Tom40, pb_2(220)dc1-Tom40, or pb_2(220)dc2-Tom40 exhibited the final TOM40 complex, although in varying amounts (Figure 6C), suggesting that all the pb_2(220)-Tom40 variants were correctly assembled into the TOM40 complex. The decreased amount of pb_2(220)dc2-Tom40 in the final TOM40 complex (Figure 6C) is consistent with the retarded growth rate of the strain expressing pb_2(220)dc2-Tom40 at 37°C (Figure 6A). Taking these results together, we conclude that pb_2(220)-Tom40, pb_2(220)AA-Tom40, pb_2(220)dc1-Tom40, and pb_2(220)dc2-Tom40, but not pb_2(220)Δ19-Tom40 or pSu9-Tom40, can be assembled into the TOM40 complex and are functional in vivo. However this in turn means that pb_2(220)AA-Tom40, which remained as the assembly

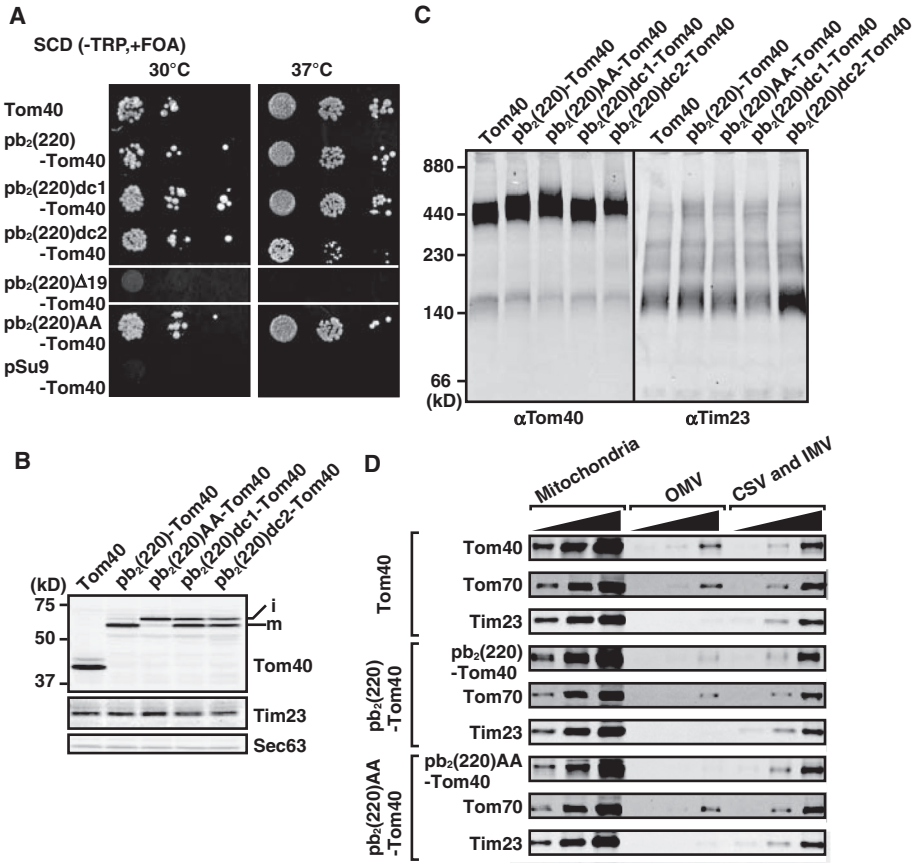

FIGURE 6: pb$_2$(220)-Tom40, pb$_2$(220)AA-Tom40, pb$_2$(220)dc1-Tom40, and pb$_2$(220)dc2-Tom40 can form functional TOM40 complexes in vivo. (A) A *TRP1* low-copy plasmid harboring the gene for indicated proteins was introduced into a haploid strain whose chromosomal disruption of *TOM40* was complemented with a *URA3* plasmid with the *TOM40* gene. Yeast cells dependent on the genes for pb$_2$(220)-Tom40 derivatives or pSu9-Tom40 on the *TRP1* plasmids were selected on 5′-FOA plates (SCD, –TRP) by drop dilution test with 10-fold increments at 30 and 37°C. (B) Total lysates were prepared from the yeast stains whose chromosomal disruption of *TOM40* was complemented with a *TRP1* plasmid harboring the gene for Tom40, pb$_2$(220)-Tom40, pb$_2$(220)AA-Tom40, pb$_2$(220)dc1-Tom40, or pb$_2$(220)dc2-Tom40. Proteins were analyzed by SDS–PAGE and immunoblotting with antibodies against indicated proteins. i, intermediate-size form; m, mature-size form. (C) Mitochondria were prepared from the indicated yeast strains as in B, solubilized with 1% digitonin, and subjected to BN-PAGE. Proteins were detected by immunoblotting with antibodies against Tom40 (αTom40) and Tim23 (αTom23). (D) Submitochondrial membrane vesicles were prepared by sonication of mitochondria with Tom40, pb$_2$(220)-Tom40, or pb$_2$(220)AA-Tom40 (as in C). Outer membrane vesicles (OMVs) were separated from inner-membrane vesicles (IMVs) and contact-site vesicles (CSVs; tethered outer and inner membrane vesicles) by 0.85–1.6 M sucrose density gradient centrifugation. Proteins (with threefold increments) from mitochondria before sonication (Mitochondria), the fraction containing OMV, and that containing CSV + IMV were analyzed by SDS–PAGE and immunoblotting with antibodies against Tom40, Tom70, and Tim23.

intermediate I even after 90 min of incubation in vitro, is assembled into the final TOM40 complex in vivo. This raises the question of whether the presequence of pb$_2$(220)AA-Tom40 is still anchored to the inner membrane in vivo. We thus disrupted mitochondria with WT Tom40, pb$_2$(220)-Tom40, and pb$_2$(220)AA-Tom40 by sonication and subjected the resultant vesicles to density gradient centrifugation to separate fractions containing outer-membrane vesicles from those with contact-site and inner-membrane vesicles (Pon *et al.*, 1989). Although Tom40 and pb$_2$(220)-Tom40 were found in both the outer-membrane vesicle fraction and the contact-site plus inner-membrane vesicle fraction, pb$_2$(220)AA-Tom40 was exclusively found in the fraction containing contact-site and inner-membrane vesicles and not in the fraction with outer-membrane vesicles (Figure 6D). We also used quantitative immuno–electron microscopy (EM) analyses to examine the distribution of Tom40 or its derivatives within mitochondria by immunogold labeling (Figure 7). Gold particles were found in contact sites where the outer and inner membranes are in close proximity to each other, as well as in outer membranes in mitochondria expressing Tom40 or pb$_2$(220)-Tom40 (Figure 7, top and middle). In contrast, when pb$_2$(220)AA-Tom40 was expressed, the majority of the gold particles were located at contact sites with pb$_2$(220)AA-Tom40 rather than the outer mitochondrial membrane (Figure 7, bottom). Therefore, in contrast to Tom40 and pb$_2$(220)-Tom40, pb$_2$(220)AA-Tom40 is mainly located at contact sites rather than at the outer membrane. This may be due to the tethering of pb$_2$(220)AA-Tom40 to the outer and inner membranes via its Tom40 domain and presequence, respectively. In other words, the Tom40 domain of pb$_2$(220)AA-Tom40 likely integrates into the final TOM40 complex with its presequence still being anchored to the inner membrane in vivo.

DISCUSSION

In the present study, we analyzed the effects of fusing different mitochondrial sorting signals to Tom40 to assess the mechanism responsible for the sorting and assembly of Tom40 in mitochondria. For this purpose, we analyzed the in vitro import of fusion proteins containing various mitochondrial presequences with sorting signals for the IMS, inner membrane, and matrix. The suggested sorting and assembly pathways of Tom40 and its fusion proteins are summarized in Figure 8. The results show that 1) the Tom40 assembly pathway is not independent of or separate from the inner membrane or IMS-sorting pathway, 2) both pathways may be active during import, which would allow the N-terminal presequences and C-terminal Tom40 domain to follow their inherent sorting pathways, and 3) the requirement of the components, for example, the small Tim proteins, for one pathway can be circumvented by commitment to the other pathway.

pb$_2$(220)-Tom40 with the WT cytochrome b_2 presequence followed the targeting pathway of cytochrome b_2 for translocation from the N-terminus through the TOM40 channel and partial insertion into the TIM23 channel. After cleavage of the N-terminal part of the presequence by MPP in the matrix and translocation of the Tom40 part across the outer membrane, the presequence and Tom40 part of pb$_2$(220)-Tom40 followed their distinct sorting pathways independently of each other. The C-terminal part of the presequence was laterally released from the TIM23 complex to the inner membrane and processed by Imp1, whereas the Tom40 part associated with the

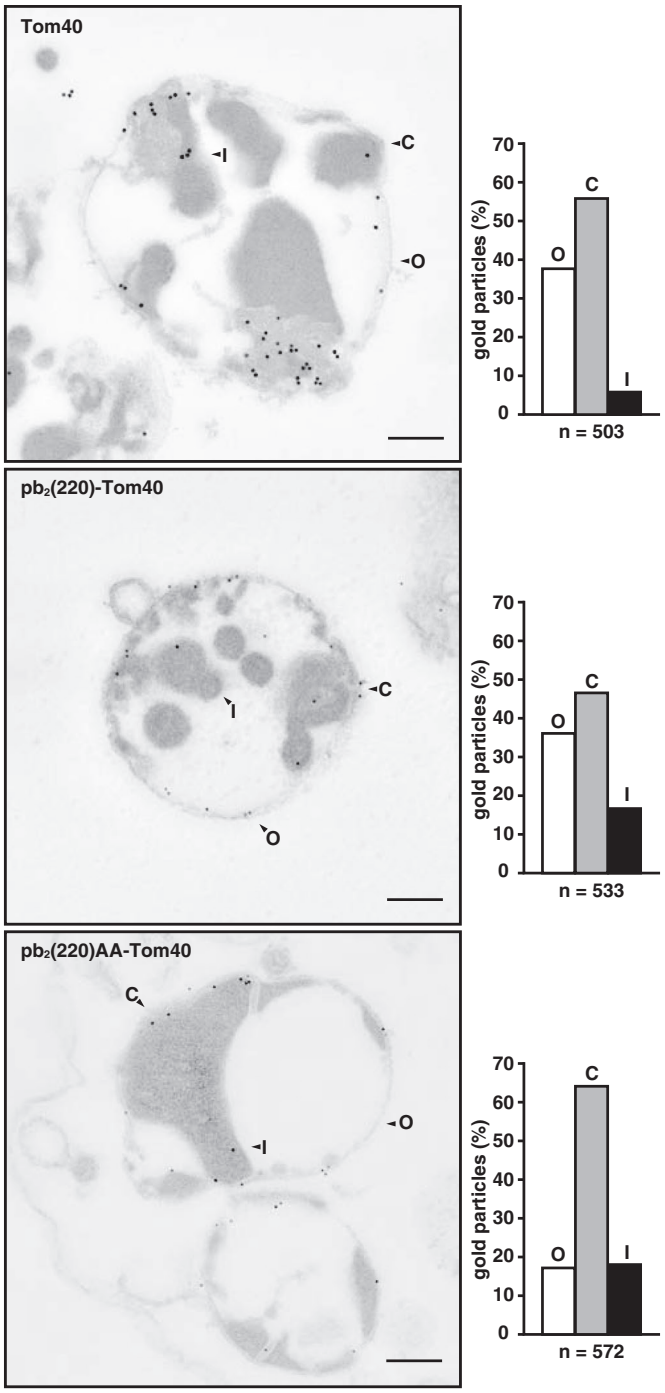

FIGURE 7: pb_2(220)AA-Tom40 is predominantly localized at mitochondrial contact sites. Distribution of Tom40 (top), pb_2(220)-Tom40 (middle), or pb_2(220)AA-Tom40 (bottom) in the mitochondria by immuno-EM analysis using the anti-Tom40 antibody. Left, representative image. Right, quantification of the Tom40, pb_2(220)-Tom40, or pb_2(220)AA-Tom40 distributed in the outer membrane, contact-site membrane, and inner membrane. C, contact-site membrane; I, inner membrane; O, outer membrane. Scale bars, 200 nm. *n*, total number of gold particles analyzed.

TOB complex to form the assembly I intermediate, subsequently shifted to the assembly II intermediate, and finally assembled into the TOM40 complex. Although the presequence of pb_2(220)-Tom40 was cleaved off by Imp1 in the IMS, the remaining cytochrome b_2 part still contained the HBD, which was tightly folded, as indicated by the efficient Imp1 processing of the presequence (Esaki *et al.*, 1999). Therefore the tightly folded HBD at the N-terminus of Tom40 does not interfere with the correct assembly of Tom40 via the assembly I and II intermediates.

On the other hand, although the presequence with the AA mutation, which anchored the passenger protein to the inner membrane permanently, allowed Tom40 to partly form the assembly I intermediate with the TOB complex, further release from the TOB complex was significantly inhibited in vitro but not in vivo. Therefore the free N-terminus is essential for Tom40 to dissociate from, but not to associate with, the TOB complex efficiently at least in vitro. In contrast to pb_2(220)AA-Tom40, the cytochrome b_2 presequence with the dc1 or dc2 mutation, which retarded Imp1 cleavage, allowed Tom40 to leave the TOB complex slowly to form the assembly II intermediate and subsequently the final TOM40 complex in vitro. This observation again points to the importance of the cleavage of the C-terminal half of the presequence anchored to the inner membrane by Imp1 for the efficient release of Tom40 from the TOB complex in vitro. Because the presequence cleavage by Imp1 can take place slowly at the inner membrane, this indicates that Tom40 can associate with the TOB complex while still being anchored to the inner membrane by the presequence.

Next we found that the small Tim-dependent step of the assembly of the Tom40 in the outer membrane can be substituted by IMS sorting guided by the cytochrome b_2 presequence. Although small Tim proteins in the IMS were found to be involved in the early steps of the Tom40 assembly (Hoppins and Nargang, 2004; Wiedemann *et al.*, 2004), their precise roles have remained elusive. Depletion of Tim10 did not significantly affect translocation of pb_2(220)-Tom40 across the outer membrane, whereas accumulation of the assembly I intermediate was, like that of Tom40, markedly reduced in the absence of Tim10. These results suggest that when the cytochrome b_2 presequence is present, small Tim proteins are no longer required for the translocation of Tom40 across the outer membrane. Small Tim proteins likely drive translocation of both Tom40 and inner membrane carrier proteins across the outer membrane by trapping the incoming unfolded polypeptide segment in the IMS, thereby preventing their retrotranslocation through the TOM40 channel. Because the cytochrome b_2 presequence can pull in the passenger domain across the outer membrane by the anchor-diffusion mechanism (Esaki *et al.*, 1999), the cytochrome b_2 presequence in pb_2(220)-Tom40 could drive the translocation of Tom40 across the outer membrane. On the other hand, the pb_2(220) segment (in the presence of $\Delta\Psi$) cannot fulfill the role of small Tim proteins in stabilizing the association of Tom40 with the TOB complex. Small Tim proteins may function as chaperones to keep Tom40 soluble in the IMS, which is important for efficient and stable interactions with the TOB complex (Habib *et al.*, 2007).

The matrix-targeting presequences of Δ19 cytochrome b_2 and pSu9 presequences directed Tom40 predominantly to the matrix. When complete presequence translocation through the TIM23 channel is blocked by dissipation of $\Delta\Psi$, the Tom40 assembly pathway is reactivated, that is, Tom40 can now cross the outer membrane independently of small Tim proteins and enter the assembly pathway as long as the distance between the presequence and Tom40 part is not too large. This is supported by the observation that, in the absence of $\Delta\Psi$, the mature part adjacent to the presequence (in the case of pSu9-Tom40 and pb_2(80)Δ19-Tom40 but not of pb_2(165)-Tom40 or pb_2(220)Δ19-Tom40) can become unfolded and trapped by the Tom40 channel, and such association with the TOM40 complex is sufficient for the Tom40 part to

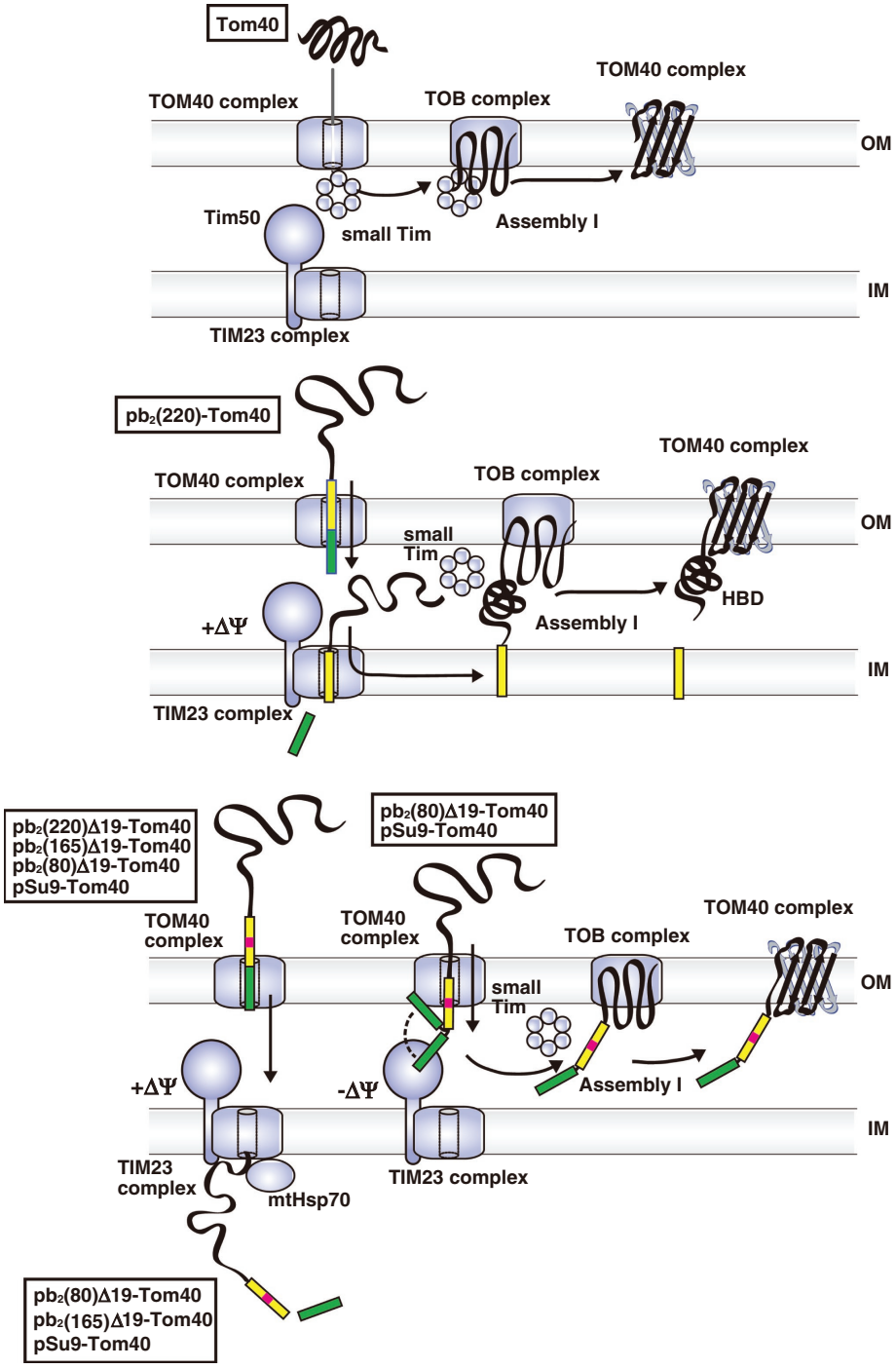

FIGURE 8: Assembly pathways of Tom40 and Tom40 fusion proteins. Assembly pathways of Tom40 (top), pb_2(220)-Tom40 (middle), pb_2(220)Δ19-Tom40, pb_2(165)Δ19-Tom40, or pb_2(80)Δ19-Tom40 in the presence of ΔΨ (bottom, +ΔΨ), and pb_2(80)Δ19-Tom40 or pSu9-Tom40 in the absence of ΔΨ (bottom, −ΔΨ; presequence of pb_2(80)Δ19-Tom40, not pSu9-Tom40 is shown) are schematically shown. The assembly II forms were omitted for simplicity. Green box and yellow box, the N-terminal part and C-terminal part of the cytochrome b_2 presequence with a matrix-targeting signal and a IMS sorting signal, respectively; yellow box with a pink bar, inactivated sorting signal. IM, inner membrane; mtHsp70, mitochondrial Hsp70; OM, outer membrane.

follow its import and subsequent assembly pathway in the outer membrane.

We also compared the effects of cytochrome b_2–derived and other presequences on the assembly process of Tom40 in vitro and in vivo. The inability of pb_2(220)Δ19-Tom40 and pSu9-Tom40 to rescue the growth defects caused by *TOM40* disruption is consistent with the in vitro observation that pb_2(220)Δ19-Tom40 and pSu9-Tom40 failed to assemble into the TOM40 complex in the outer membrane. The ability of pb_2(220)-Tom40, pb_2(220)dc1-Tom40, and pb_2(220)dc2-Tom40 to rescue the *TOM40* disruption is also supported by the observation that they followed the normal assembly pathway of Tom40 in vitro and were successfully assembled into the TOM40 complex. Unexpectedly, pb_2(220)AA-Tom40, which formed only a small amount of the final TOM40 complex in vitro, rescued the growth defects caused by the *TOM40* disruption. This indicates that the slow and inefficient assembly of newly synthesized pb_2(220)AA-Tom40 into the TOM40 complex may still be sufficient to maintain the necessary amounts of the functional TOM40 complex that accumulate at the contact sites of mitochondria in vivo. Alternatively, the present assembly process of Tom40 observed in vitro may be much more inefficient than that in vivo because it took longer than 1 h for Tom40 to become functional in vitro, which is long compared with the yeast doubling time of 2–3 h. In addition, the in vitro assay system for Tom40 assembly may lack factor(s) that accelerate the assembly process. The identification of such factor(s) will be an important subject for future studies.

MATERIALS AND METHODS

Plasmids

The plasmids used in this study are described in Supplemental Tables S1 and S2. In vitro translation of pb_2(220)-Tom40 and its derivatives (Δ19, dc1, dc2, and AA) were done as follows. DNA fragments encoding the N-terminal 220 amino acid residues of the cytochrome b_2 precursor and those with mutations of Δ19, dc1, dc2, or AA were amplified from pGEM-pb_2(220)-DHFR and its derivatives (Esaki *et al.*, 1999) by PCR, digested with *Eco*RI and *Sac*I, and inserted into pGEM-4Z (Promega, Madison, WI), resulting in pGEM-pb_2(220) and its derivatives, respectively. A DNA fragment encoding the *TOM40* gene, with the first Met codon replaced by the one for Ala, was amplified from pGEM-Tom40 (Ishikawa *et al.*, 2004) by PCR, digested with *Sac*I and *Sal*I, and inserted into the pGEM-pb_2(220) and its derivatives, resulting in pGEM-pb_2(220)-Tom40 and its derivatives, respectively.

The plasmids used for in vitro translation of pb2(80)Δ19-Tom40 and pb_2(165)Δ19-Tom40 were constructed as follows. DNA fragments encoding the N-terminal 80 or 165 amino acid residues with Δ19 of the cytochrome b_2 precursor were amplified from

pGEM-pb_2(220)Δ19-Tom40 by PCR, digested with *Eco*RI and *Sac*I, and inserted into pGEM-4Z, resulting in pGEM-pb_2(80)Δ19 or pGEM-pb_2(165)Δ19, respectively. A DNA fragment encoding the *TOM40* gene with the first Met codon replaced by the one for Ala was digested with *Sac*I and *Sal*I from pGEM-pb_2(220)-Tom40 and inserted into pGEM-pb_2(80)Δ19 or pGEM-pb_2(165)Δ19, resulting in pb_2(80)Δ19-Tom40 and pb_2(165)Δ19-Tom40, respectively.

The plasmid used for in vitro translation of pSu9-Tom40 was constructed as follows. A DNA fragment (fragment F) encoding the N-terminal 69 amino acid residues of the precursor to subunit 9 of F_0-ATPase of *Neurospora crassa* flanked by its 5′-untranslated region (UTR; 30 base pairs) and the first 13 base pairs of the *Saccharomyces cerevisiae TOM40* gene, with the first Met codon replaced by the one for Ala, was amplified from the plasmid pGEM-pSu9-DHFR by PCR. A DNA fragment (fragment R) encoding the *TOM40* gene, with the first Met codon replaced by the one for Ala, following the last 13 base pairs of the sequence encoding the 69 amino acid residues presequence of subunit 9 of F_0-ATPase was amplified from pGEM-4Z-pb_2(220)-DHFR by PCR. A DNA fragment encoding pSu9-Tom40 with the 5′-UTR (30 base pairs) of subunit 9 of F_0-ATPase was amplified by PCR using fragments F and R as templates and *Bam*HI-pSu9(-30)-F and Su9-Tom40-R as primers, digested with *Bam*HI and *Sal*I, and inserted into pGEM-4Z, resulting in pGEM-pSu9-Tom40.

The plasmids used for in vitro translation of pSu9-Tom40His_{10} and pSu9-Tom40FLAG were constructed as follows. DNA fragments encoding the C-terminal 23 amino acid residues of Tom40 with the His_{10} tag or FLAG tag were amplified from pGEM-Tom40 by PCR, digested with *Xba*I and *Sal*I, and inserted into pGEM-pSu9-Tom40, resulting in pSu9-Tom40His_{10} or pSu9-Tom40FLAG, respectively.

Yeast strains and growth conditions

Yeast strains used in this study are described in Supplemental Table S3. Yeast haploid strains expressing pb_2(220)-Tom40 and its derivatives (Δ19, dc1, dc2, and AA) or pSu9-Tom40 under the *CUP1* promoter from a *CEN6-TRP1* plasmid pTYSC124 (a gift from T. Yoshihisa, Nagoya University) instead of wild-type Tom40 on the chromosomal DNA were constructed as follows. DNA fragments encoding pb_2(220)-Tom40 and its derivatives were amplified from the plasmid pGEM-pb_2(220)-Tom40 or its derivatives by PCR using primers BglII-pb2 and Tom40-SacII (Supplemental Table S4), digested with *Bgl*II and *Sac*II, and inserted into pTYSC124, resulting in pTYSC124-pb_2(220)-Tom40 and its derivatives. A DNA fragment encoding pSu9-Tom40 was amplified from the plasmid pGEM-pSu9-Tom40 by PCR using primers *Bgl*II-pSu9 and Tom40-*Sac*II; Supplemental Table S2), digested with *Bgl*II and *Sac*II, and inserted into pTYSC124-pb2(220)-Tom40, resulting in pTYSC124-pSu9-Tom40. W303-isp42/A1 was transformed with pTYSC124-pb_2(220)-Tom40, its derivatives, or pTYSC124-pSu9-Tom40, and the resulting Trp^+ transformants were selected for Ura^- colonies by 5′-FOA.

Yeast cells were grown in lactate medium (0.3% yeast extract, 0.05% glucose, 2% lactic acid, pH 5.6), lactate (+1% glucose) medium (0.3% yeast extract, 1% glucose, 2% lactic acid, pH 5.6), lactate (+1% galactose) medium (0.3% yeast extract, 1% galactose, 2% lactic acid, pH 5.6), SCD (0.67% yeast nitrogen base without amino acids, 0.5% casamino acids, 2% glucose), YPD (1% yeast extract, 2% polypeptone, 2% glucose), or YPLac (1% yeast extract, 2% polypeptone, 2% lactic acid) with appropriate supplements (Rose *et al.*, 1990).

Electron microscopy analyses

Mitochondria were isolated from yeast cells after cultivation in SCD (–Trp) medium at 30°C, incubated in buffer S (1.2 M sorbitol, 20 mM 4-(2-hydroxyethyl)-1-piperazineethanesulfonic acid [HEPES]-KOH, pH 7.4) for 10 min at 4°C, and fixed by incubation in buffer S containing 0.5% glutaraldehyde and 3% paraformaldehyde for 2 h at 0°C. After several washes, samples were dehydrated in ethanol and embedded in LR White resin. Ultrathin 70-nm sections were cut with a diamond knife on an ultramicrotome (2088 Ultrotome V; LKB/Pharmacia Fine Chemicals, Uppsala, Sweden) and prepared for immunolabeling immediately afterward. The ultrathin sections were incubated with the anti-Tom40 monoclonal mouse antibody (T. Kanamori and S. Nishikawa, Nagoya University, unpublished data) for 12 h at 4°C. After washing, the ultrathin sections were incubated for 1 h in 10-nm gold-conjugated goat anti-mouse immunoglobulin G and fixed with glutaraldehyde to stabilize the gold particles. Samples were stained with 2% uranyl acetate and lead citrate and then examined in a JEM-1200EX electron microscope (JEOL, Tokyo, Japan).

For quantification, submitochondrial locations of at least 500 individual gold particles were analyzed. To determine the relative surface areas of the outer membrane, the contact-site membrane, and the inner membrane, representative images showing sufficient structural preservation were chosen, and the membrane length was measured by using ImageJ (National Institutes of Health, Bethesda, MD). Gold particles within <10 nm of the membrane were assigned to membrane proteins. Assignments of the outer membrane, contact-site membrane, and inner membrane were as described (Pon *et al.*, 1989).

Miscellaneous

Import of radiolabeled precursor proteins translated in vitro into D273-10B mitochondria, BN-PAGE, and immunoblotting was performed as described previously (Schägger, 2001; Yamamoto *et al.*, 2002; Ishikawa *et al.*, 2004; Tamura *et al.*, 2006).

Submitochondrial membrane vesicles were produced and fractionated as described (Pon *et al.*, 1989). Briefly, isolated mitochondria (10–15 mg of protein) were suspended to 1 mg/ml in 10 mM Tris-PO_4, pH 7.4, and 1 mM phenylmethylsulfonyl fluoride and incubated for 30 min on ice for swelling. After addition of 0.45 M sucrose, 2 mM $MgCl_2$, and 2 mM ATP, the mitochondria were further incubated for 10 min on ice and subsequently sonicated with an Astrason Ultrasonic Processor (Heat Systems-Ultrasonic, Misonix, Farmingdale, NY). The sonicated mixture was clarified by centrifugation at 30,000 × *g* for 20 min at 4°C, and submitochondrial membrane vesicles in the supernatant were collected by centrifugation at 200,000 × *g* for min at 4°C. The membrane vesicles were resuspended in 5 mM HEPES/KOH, pH 7.4, 10 mM KCl, and 1 mM $MgCl_2$, layered onto discontinuous sucrose gradient (1.25 ml each of 1.6, 1.35, 1.1, and 0.85 M sucrose in 5 mM HEPES/KOH, pH 7.4, 10 mM KCl, and 1 mM $MgCl_2$), and centrifuged at 135,000 × *g* for 15 h at 4°C.

ACKNOWLEDGMENTS

We thank members of the Endo lab for discussions. Y.T. and T.S. are Research Fellows of the Japan Society for the Promotion of Science. This study was supported in part by Grants-in-Aid for Scientific Research from the Ministry of Education, Science, Sports and Culture of Japan and a grant from the Japan Science and Technology Corporation.

REFERENCES

Abe Y, Shodai T, Muto T, Mihara K, Torii H, Nishikawa S, Endo T, Kohda D (2000). Structural basis of presequence recognition by the mitochondrial protein import receptor Tom20. Cell 100, 551–560.

Ahting U, Thieffry N, Engelhardt H, Hegerl R, Neupert W, Nussberger S (2001). Tom40, the pore-forming component of the protein-conducting

TOM channel in the outer membrane of mitochondria. J Cell Biol 153, 1151–1160.
Brix J, Rüdiger S, Bukau B, Schneider-Mergener J, Pfanner N (1999). Distribution of binding sequences for the mitochondrial import receptors Tom20, Tom22, and Tom70 in a presequence-carrying preprotein and a non-cleavable preprotein. J Biol Chem 274, 16522–16530.
Chacinska A, Koehler CM, Milenkovic D, Lithgow T, Pfanner N (2009). Importing mitochondrial proteins: machineries and mechanisms. Cell 138, 628–644.
Endo T, Yamano K (2009). Multiple pathways for mitochondrial protein traffic. Biol Chem 390, 723–730.
Esaki M, Kanamori T, Nishikawa S, Endo T (1999). Two distinct mechanisms drive protein translocation across the mitochondrial outer membrane in the late step of the cytochrome b_2 import pathway. Proc Natl Acad Sci USA 96, 11770–1177.
Gentle I, Gabriel K, Beech P, Waller R, Lithgow T (2004). The Omp85 family of proteins is essential for outer membrane biogenesis in mitochondria and bacteria. J Cell Biol 164, 19–24.
Glick BS, Brandt A, Cunningham K, Müller S, Hallberg RL, Schatz G (1992). Cytochrome c_1 and b_2 are sorted to the intermembrane space of yeast mitochondria by a stop-transfer mechanism. Cell 69, 809–822.
Habib SJ, Waizenegger T, Niewienda A, Paschen SA, Neupert W, Rapaport D (2007). The N-terminal domain of Tob55 has a receptor-like function in the biogenesis of mitochondrial β-barrel proteins. J Cell Biol 176, 77–88.
Hill K, Model K, Ryan MT, Dietmeier K, Martin F, Wagner R, Pfanner N (1998). Tom40 forms the hydrophobic channel of the mitochondrial import pore for preproteins. Nature 395, 516–521.
Hoppins SC, Nargang FE (2004). The Tim8-Tim13 complex of *Neurospora crassa* functions in the assembly of proteins into both mitochondrial membranes. J Biol Chem 279, 12396–12405.
Imai K, Gromiha MM, Horton P (2008). Mitochondrial β-barrel proteins, an exclusive club? Cell 135, 1158–1159.
Ishikawa D, Yamamoto H, Tamura Y, Moritoh K, Endo T (2004). Two novel proteins in the mitochondrial outer membrane mediate β-barrel protein assembly. J Cell Biol 166, 621–627.
Kanamori T, Nishikawa S, Nakai M, Shin I, Schultz PG, Endo T (1999). Uncoupling of transfer of the presequence and unfolding of the mature domain in precursor translocation across the mitochondrial outer membrane. Proc Natl Acad Sci USA 96, 3634–3639.
Koehler CM, Jarosch E, Tokatlidis K, Schmid K, Schweyen RJ, Schatz G (1998). Import of mitochondrial carriers mediated by essential proteins of the intermembrane space. Science 279, 369–373.
Kornmann B, Currie E, Collins SR, Schuldiner M, Nunnari J, Weissman JS, Walter P (2009). An ER-mitochondria tethering complex revealed by a synthetic biology screen. Science 325, 477–481.
Kozjak V, Wiedemann N, Milenkovic D, Lohaus C, Meyer HE, Guiard B, Meisinger C, Pfanner N (2003). An essential role of Sam50 in the protein sorting and assembly machinery of the mitochondrial outer membrane. J Biol Chem 278, 48520–48523.
Meisinger C *et al*. (2004). The mitochondrial morphology protein Mdm10 functions in assembly of the preprotein translocase of the outer membrane. Dev Cell 7, 61–71.
Milenkovic D, Kozjak V, Wiedemann N, Lohaus C, Meyer HE, Guiard B, Pfanner N, Meisinger C (2004). Sam35 of the mitochondrial protein sorting and assembly machinery is a peripheral outer membrane protein essential for cell viability. J Biol Chem 279, 22781–22785.
Model K, Meisinger C, Prinz T, Wiedemann N, Truscott KN, Pfanner N, Ryan MT (2001). Multistep assembly of the protein import channel of the mitochondrial outer membrane. Nat Struct Biol 8, 361–370.
Momose T, Ohshima C, Maeda M, Endo T (2007). Structural basis of functional cooperation of Tim15/Zim17 with yeast mitochondrial Hsp70. EMBO Rep 8, 664–670.
Neupert W, Herrmann JM (2007). Translocation of proteins into mitochondria. Annu Rev Biochem 76, 723–749.
Paschen SA, Neupert W, Rapaport D (2005). Biogenesis of β-barrel membrane proteins of mitochondria. Trends Biochem Sci 30, 575–582.
Paschen SA, Waizengger T, Stan T, Preuss M, Cyklaff M, Hell K, Rapaport D, Neupert W (2003). Evolutionary conservation of biogenesis of β-barrel membrane proteins. Nature 426, 862–866.
Pfanner N, Wiedemann N, Meisinger C, Lithgow T (2004). Assembling the mitochondrial outer membrane. Nat Struct Mol Biol 11, 1044–1048.
Pon L, Moll T, Vestweber D, Marshallsay B, Schatz G (1989). Protein import into mitochondria: ATP-dependent protein translocation activity in a submitochondrial fraction enriched in membrane contact sites and specific proteins. J Cell Biol 109, 2603–2616.
Rose MD, Winston F, Hieter P (1990). Methods in Yeast Genetics: A Laboratory Course Manual, Cold Spring Harbor, NY: Cold Spring Harbor Laboratory Press.
Schägger H (2001). Blue-native gels to isolate protein complexes from mitochondria. In: Mitochondria, ed. LA Pon and EA Schon, San Diego, CA: Academic Press, 231–244.
Sichting M, Mokranjac D, Azem A, Neupert W, Hell K (2005). Maintenance of structure and function of mitochondrial Hsp70 chaperones requires the chaperone Hep1. EMBO J 24, 1046–1056.
Sirrenberg C, Endres M, Fölsch H, Stuart RA, Neupert W, Brunner M (1998). Carrier protein import into mitochondria mediated by the intermembrane proteins Tim10/Mrs11 and Tim12/Mrs5. Nature 391, 912–915.
Tamura Y, Harada Y, Shiota T, Yamano K, Watanabe K, Yokota M, Yamamoto H, Sesaki H, Endo T (2009). Tim23-Tim50 pair coordinates functions of translocators and motor proteins in mitochondrial protein import. J Cell Biol 184, 129–141.
Tamura Y, Harada Y, Yamano K, Watanabe K, Ishikawa D, Ohshima C, Nishikawa S, Yamamoto H, Endo T (2006). Identification of Tam41 maintaining integrity of the TIM23 protein translocator complex in mitochondria. J Cell Biol 174, 631–637.
Waizenegger T, Habib SJ, Lech M, Mokranjac D, Paschen SA, Hell K, Neupert W, Rapaport D (2004a). Tob38, a novel essential component in the biogenesis of β-barrel proteins of mitochondria. EMBO Rep 5, 704–709.
Waizenegger T, Schmitt S, Zivkovic J, Neupert W, Rapaport D (2004b). Mim1, a protein required for the assembly of the TOM complex of mitochondria. EMBO Rep 6, 57–62.
Wiedemann N, Kozjak V, Chacinska A, Schönfisch B, Rospert S, Ryan MT, Pfanner N, Meisinger C (2003). Machinery for protein sorting and assembly in the mitochondrial outer membrane. Nature 424, 565–571.
Wiedemann N, Truscott KN, Pfannschmidt S, Guiard B, Meisinger C, Pfanner N (2004). Biogenesis of the protein import channel of Tom40 of the mitochondrial outer membrane. Intermembrane space components are involved in an early stage of the assembly pathway. J Biol Chem 279, 18188–18194.
Yamamoto H, Esaki M, Kanamori T, Tamura Y, Nishikawa S, Endo T (2002). Tim50, a new subunit of the TIM23 complex that links mitochondrial protein translocation across the outer and inner mitochondrial membranes. Cell 111, 519–528.
Yamano K, Ishikawa D, Esaki M, Endo T (2005). The phosphate carrier has an ability for be sorted to either the TIM22 pathway or the TIM23 pathway for its import into yeast mitochondria. J Biol Chem 280, 10011–10017.
Yamano K, Tanaka-Yamano S, Endo T (2010a). Mdm10 as a dynamic constituent of the TOB/SAM complex directs coordinated assembly of Tom40. EMBO Rep 11, 187–193.
Yamano K, Tanaka-Yamano S, Endo T (2010b). Tom7 regulates Mdm10-mediated assembly of the mitochondrial import channel protein Tom40. J Biol Chem 285, 41222–41231.